PROCEEDINGS OF SCIENCE

Searches for New Physics in final states with leptons or photons with CMS

Jan-Frederik Schulte[a,1,*]
[a] *Purdue University, West Lafayette, IN, USA*
E-mail: jschulte@cern.ch

Searches for new physics with leptons and photons in the final state have a long tradition at collider experiments, as they offer clean final states that allow to efficiently select signals of potential new physics while controlling backgrounds from standard model processes. As the search program of the CMS experiment matures, analyses are expanding to cover new final states, use novel analyses techniques, or recast the results of more traditional approaches to extract more information from the collected data sets. Here, four recent searches using the full data set collected by CMS during the LHC Run 2 are discussed, ranging from simple dilepton final states to searches for $W\gamma$ resonances and Dark Higgs particles decaying to W bosons.

**** The European Physical Society Conference on High Energy Physics (EPS-HEP2021), ****
**** 26-30 July 2021 ****
**** Online conference, jointly organized by Universität Hamburg and the research center DESY ****

[1]For the CMS collaboration.
*Speaker

PoS(EPS-HEP2021)680

The search for new physics beyond the standard model (SM) of particle physics is one of the main objectives of the experiments at the CERN LHC. One of the strengths of the CMS detector [1] is its ability to trigger, reconstruct, and identify leptons and photons with high efficiency and precision. Selecting events containing these particles therefore allows to efficiently select the small signals of new physics while reducing background form SM processes.

After over a decade of searches for new physics at the LHC, many searches have reached a mature state and are approaching the limit of their discovery reach at the center of mass energy of $\sqrt{s}$ = 13 TeV, so that a significant increase in integrated luminosity is necessary to significantly improve their sensitivity. New analyses targeting new physics models hitherto uncovered or employing novel analysis techniques are therefore launched while established analyses are branching out into new interpretations to extract as much information possible from the recorded data. Four recent results are presented here, each using the full dataset collected during the LHC Run 2, corresponding to $\approx 140\,\text{fb}^{-1}$.

New physics is searched for in events with two high energetic electrons or muons in the final state [2]. Fig. 1 shows the dielectron and dimuon invariant mass spectra, comparing data to the estimated event yield from SM backgrounds. These estimates are mostly derived from simulation, corrected to the highest available precision using mass dependent correction factors in case of the dominant Drell–Yan (DY) background. Good agreement is observed, except for a small excess of events at high mass in the electron channel.

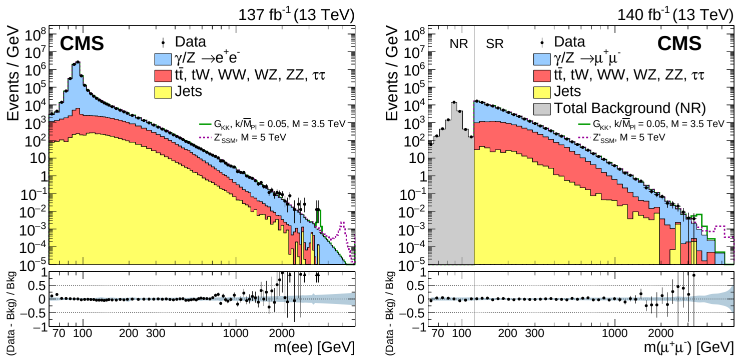

Figure 1: Dielectron (left) and dimuon (right) invariant mass distribution for the full Run 2 dataset. Data are compared to backgrounds from SM processes and two signal models are shown for illustration [2].

Limits are set on a variety of physics models predicting both resonant and nonresonant signatures. Fig 2 (left) shows the limit on the product of production cross section and branching fraction as a function of the mass of a narrow spin-1 resonance Z'. The lower mass limit reaches 5.15 TeV in case of a Z' in the sequential standard model (SSM). Limits are also set on the mass of spin-2 resonances and spin-1 mediator particles in Dark Matter models, ranging from ≈1 to ≈5 TeV.

Limits are also set on the UV cutoff parameter in two models predicting nonresonant excesses, the ADD model of extra dimensions and a model featuring four-fermion contact interactions (CI) motivated by a hypothetical fermion substructure. Figure 2 shows these limits as a function of the chosen parameter convention in case of the ADD limit and for different assumption for the helicity configuration of the CI and the sign of its interference with the SM DY process. Limits range from 5.9 to 8.9 TeV in case of the ADD model and 24 to 36 TeV in case of the CI model.

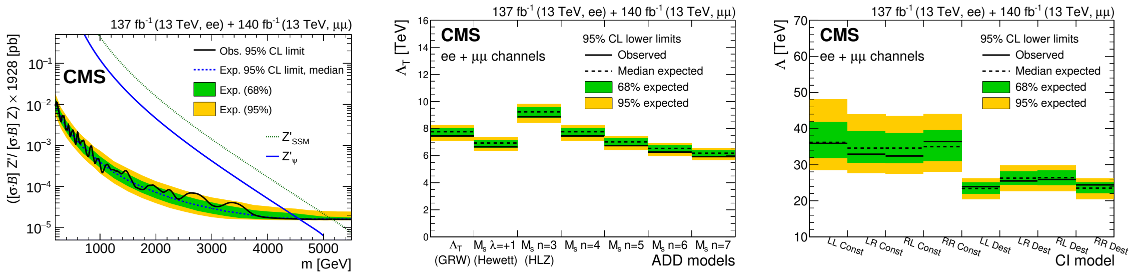

Figure 2: Left: Limit on the product of production cross section and branching fraction as a function of the Z' mass [2]. Also shown is the lower limit on the UV cutoff parameter in the ADD (center) and CI (right) models [2].

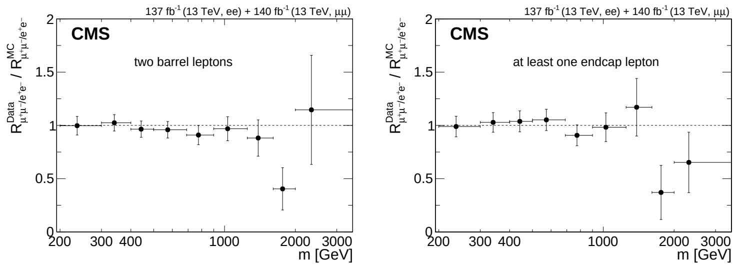

Figure 3: Ratio of the dimuon to dielectron mass spectra after unfolding and correcting the distributions to particle level. The result is shown for events with both leptons in the central part (at least one lepton in the forward part) of the detector on the left (right) [2].

Motivated by recent hints of lepton flavor universality violation, the dielectron and dimuon mass spectra are compared after unfolding for mass resolution and scale effects and correcting for the different detector acceptance and lepton efficiencies in the two channels. The result is shown in Fig. 3. The observed ratio of the dimuon to dielectron mass spectra is in good agreement with the expectation of unity, except for deviations at high mass caused by the excess of events in the dielectron channel.

Similar to the high mass dilepton search, events with one highly energetic charged lepton and large missing transverse energy E_T^{miss} are selected in another recent search, targeting decays of heavy particles into a charged lepton and a neutrino [3]. Exploiting the kinematics of this two-body decay, backgrounds are suppressed by requiring the lepton p_T and E_T^{miss} to be of roughly equal size and the two objects to be back-to-back in the transverse plane. Signals are expected to manifest as an excess at high values of the transverse mass $M_T(\ell, E_T^{miss})$. The M_T distributions in the electron and muon channels are shown in Fig. 4. SM backgrounds are estimated similarly to the dilepton search described above. Data and background are found to be in agreement in both channels.

Limits are set on the product of production cross section and branching ratio as a function of the mass of a new heavy charged gauge boson W', shown on the left side of Fig. 5. The lower limit on the W' mass in the SSM benchmark model is 5.7 TeV. To facilitate a reinterpretation of this result in different models of new physics, a limit on the product of production cross section, branching fraction, detector acceptance, and efficiency is given as a function of a lower M_T cutoff, shown in the center of Figure 5.

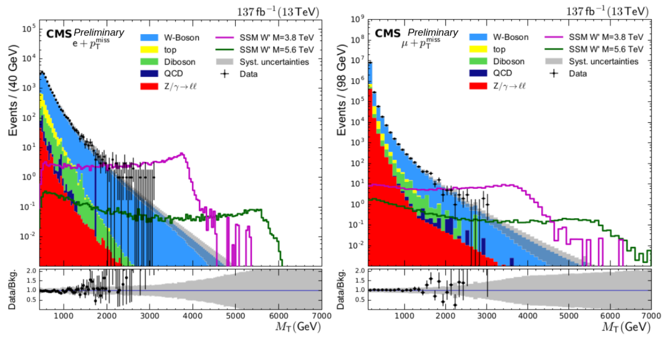

Figure 4: Distribution of the transverse mass M_{T} in electron(muon) plus E_{T}^{miss} events on the left (right).

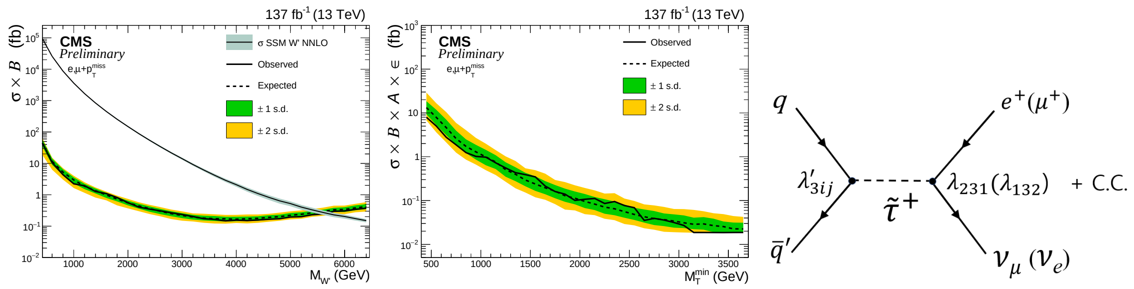

Figure 5: Limits on the product of cross section and branching fraction as a function of the mass of a hypothetical gauge boson W' (left) and limits on the product of cross section, branching ratio, acceptance, and efficiency as a function of a lower M_{T} threshold (center). Feynman diagram for the production and decay of $\tilde{\tau}$ particles via R-Parity violating couplings in a SUSY model (right) [3].

The signature of one charged lepton and a neutrino is also present in models of R-Parity violating supersymmetry (RPV SUSY), where a charged $\tilde{\tau}$ can be resonantly produced if the RPV coupling λ'_{3jj} is non-zero. The decay into the $e\nu$ ($\mu\nu$) final state is open if the couplings λ_{231} (λ_{132}) is non-zero. The Feynman diagram for this process is shown on the left side of Fig. 5. Limits are then set on the couplings λ_{231} and λ_{132} as a function of $M_{\tilde{\tau}}$ for different values of λ'_{3jj}, as shown in the middle and right plot of Fig. 6.

New particles that are too heavy to be directly produced at the LHC can nevertheless modify the M_{T} spectrum. For the first time at the LHC, this search is extended to set limits on the parameters that modify the standard model effective field theory describing these effects [4]. The high mass behavior of the W boson propagator is modified by the W parameter, to which this search is especially sensitive. Fig. 6 shows the resulting constraint in the plane of the W and Y parameters. Compared to previous results from LEP, this result significantly constrains the allowed parameter space for the W parameter, illustrating the significant amount of information that can be extracted from what might naively be considered an already fully explored final state.

Several models for new physics, such as models with extended Higgs sectors, technicolor models, or folded SUSY, predict resonances decaying to a W boson and a photon. A new search targets this final state, selecting events with hadronic decays of the W boson [5]. Given the high mass of the targeted resonances, the W bosons are highly boosted and reconstructed as single wide-radius jets, which are tagged as W boson candidates using the soft-drop jet mass and the

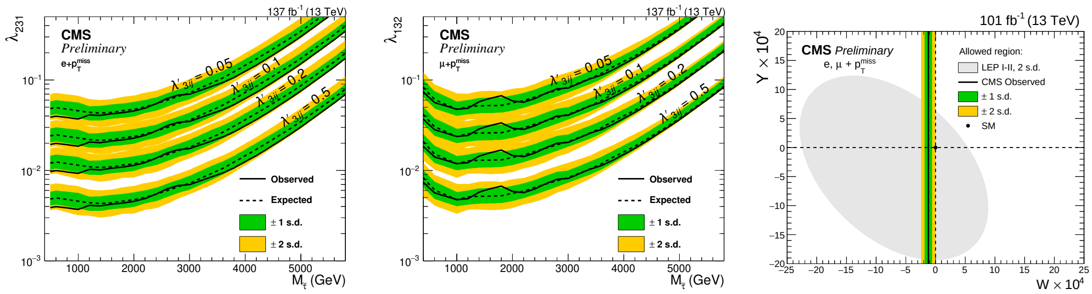

Figure 6: Limits on the RPV coupling λ_{231} (λ_{132}) as a function of $\tilde{\tau}$ mass for different values of the production coupling λ'_{3jj} for the electron (left) and muon (center) channels [3]. Also shown are constraints on the parameters W and Y in an effective field theory parameterizing deviations from the standard model effective field theory (right) [3].

N-subjettiness ratio τ_{21}. Further selection requirements are placed on η_γ, η_J, the scattering angle of the photon $\cos\theta^*_\gamma$, and the ratio of p_T^γ to $m_{\mathrm{J}\gamma}$. With this selection, a signal efficiency ranging from 6 to 12% (10-16%) is achieved for spin-0 (spin-1) resonances. Resonances are searched for the in distribution of $m_{\mathrm{J}\gamma}$, where the steeply falling background is modeled with an analytical function chosen to balance goodness-of-fit with the number of free parameters. The signal is modeled using the sum of a Crystal Ball function and one or two Gaussian functions in the case of narrow or wide resonances, respectively. The resulting $m_{\mathrm{J}\gamma}$ distribution is shown on the left side of Figure 7. The right side of the figure shows the observed local p-Value for narrow resonances and those with a relative width of 5%. The most significant deviation is observed at 1.58 TeV, where the local significance reaches 3 σ. After correcting for the look-elsewhere-effect, this reduces to 1.1-1.7 σ.

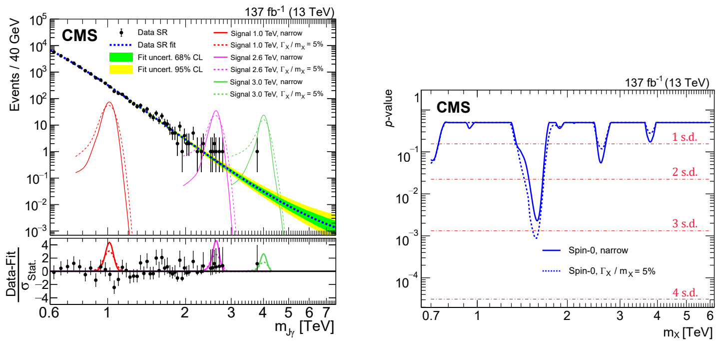

Figure 7: Left: Distribution of $m_{\mathrm{J}\gamma}$ in events with a highly boosted hadronically decaying W boson and a photon. Right: Observed local p-Value as a function of $m_{\mathrm{J}\gamma}$ for narrow and wide resonances [5].

Upper limits are set on the product of the cross section and branching fraction as a function of the resonance mass. Examples for narrow resonances are shown in Fig. 8. These are translated into lower mass limits in scalar (vector) triplet benchmark models; the limits range from 0.75-1.4 (1.15-1.35) TeV, depending on model parameters. Additionally, model independent limits on the production of cross section, branching fraction, acceptance, and efficiency are provided as a function of a lower cutoff on $m_{\mathrm{J}\gamma}$, which are also presented in Fig. 8.

In scenarios where dark matter (DM) particles acquire mass via a dark Higgs boson s, these

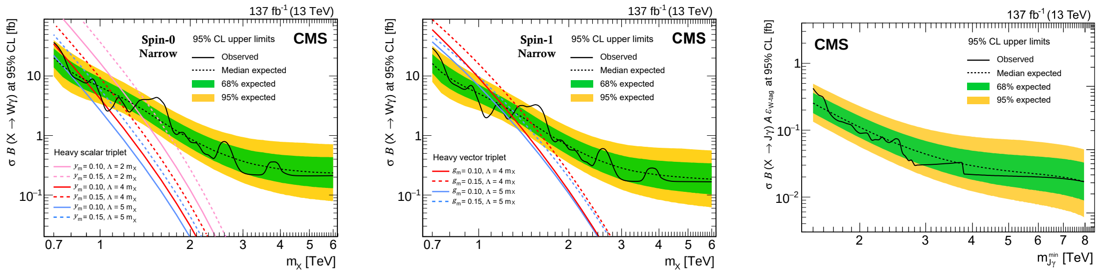

Figure 8: Upper limits on the production of cross section and branching fraction for narrow spin-0 (spin-1) resonance on the left (middle). A model independent limit on the product of cross section, branching fraction, acceptance, and efficiency as a function of a lower $m_{J\gamma}$ cutoff is shown in the right plot [5]

could be produced at the LHC in association with DM particles. The Feynman diagrams for this process is shown in Fig. 9. In a recent result, CMS searched for events where the s decay to two W bosons, which in turn decay leptonically: s $\to$ WW $\to \ell\ell\nu\nu$. Events are selected with one electron and muon of opposite charge, requiring $m_{\ell\ell} > 20$ GeV and $p_T^{\ell\ell} > 30$ GeV. SM backgrounds from WZ and ZZ production, as well as $t\bar{t}$ are rejected by vetoing third leptons and b-tagged jets. The DY background is reduced by vetoing events with same-flavor leptons and requirements on E_T^{miss} and how it aligns with the leptons.

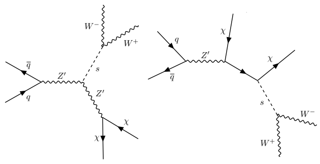

Figure 9: Feynman diagram for the production of a dark Higgs boson s decaying to W bosons in association with DM particles χ [6].

To maximize sensitivity the selected events are split into three bins in $\Delta R(\ell\ell)$, which are in turn divided into bins in $m_{\ell\ell}$ and transverse mass $M_T(\ell^{p_T,min}, E_T^{miss})$. The remaining SM backgrounds are estimated mostly from simulation, except the contribution from non-prompt leptons. Comparisons of the observed data yields with these estimates in all search bins are shown in Figure 10 and good agreement is observed.

Limits are set on the production cross section of the dark Higgs for different hypothesis of the mass of the DM particle m_χ. The limits, normalized to the signal cross section predicted from theory, are shown in the plane of the mediator mass $m_{Z'}$ and m_s in Fig. 11. The most stringent limits are set for $m_\chi = 150$ GeV, where m_s is excluded up to 300 GeV for $400 < m_{Z'} < 1200$ GeV. The highest lower limit on $m_{Z'}$ reaches 2 TeV for $m_s = 160$ GeV.

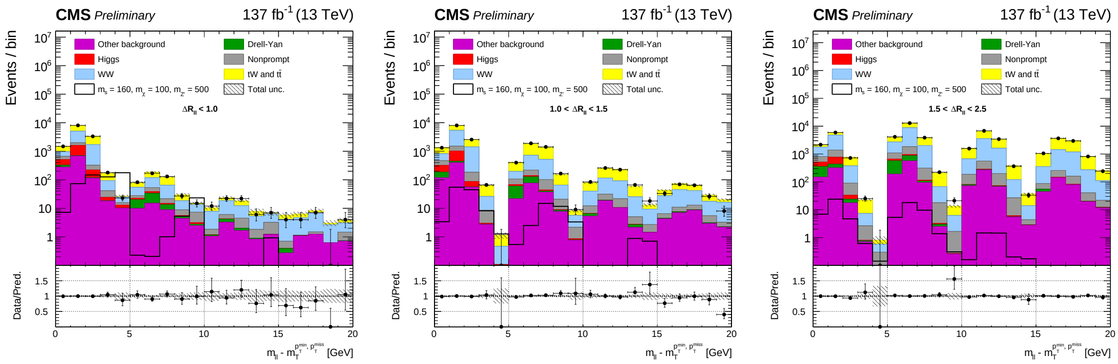

Figure 10: Observed data yields compared to expectations from SM background in all bins in $\Delta R(\ell\ell)$, $m_{\ell\ell}$, $M_{\mathrm{T}}(\ell^{p_{\mathrm{T}},min}, E_{\mathrm{T}}^{\mathrm{miss}})$ [6].

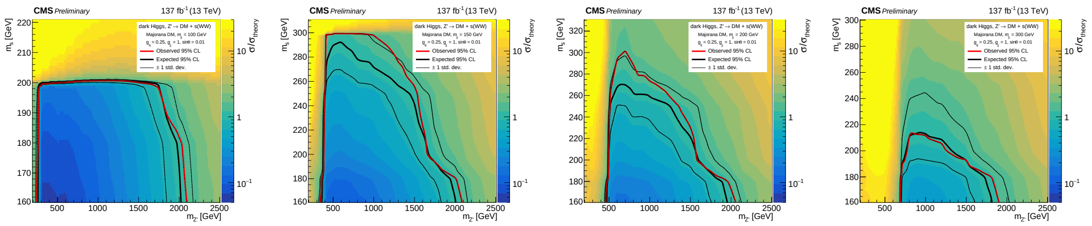

Figure 11: Cross section limit normalized to the prediction from theory in the $m_{Z'} - m_s$ plane for four different hypothesis for m_χ [6].

References

[1] CMS Collaboration, “The CMS Experiment at the CERN LHC”, JINST 3 (2008) S08004. doi:10.1088/1748-0221/3/08/S08004.

[2] CMS Collaboration, “Search for resonant and nonresonant new phenomena in high-mass dilepton final states at $\sqrt{s}$ = 13 TeV”, JHEP 07 (2021) 208. doi:10.1007/JHEP07(2021)208.

[3] CMS Collaboration, “Search for new physics in the lepton plus missing transverse momentum final state in proton-proton collisions at 13 TeV center-of-mass energy”, `CMS-PAS-EXO-19-017`, (2021).

[4] M. Farina et al., “Energy helps accuracy: electroweak precision tests at hadron colliders”, 2016, `https://arxiv.org/abs/1609.08157`.

[5] CMS Collaboration, “Search for Wγ resonances in proton-proton collisions at $\sqrt{s}$= 13 TeV using hadronic decays of Lorentz-boosted W bosons”, arxiv:2106.10509, Submitted to PLB.

[6] CMS Collaboration, “Search for new physics in the lepton plus missing transverse momentum final state in proton-proton collisions at 13 TeV center-of-mass energy”, `CMS-PAS-EXO-20-013`, (2021).